JOURNAL OF MATERIALS SCIENCE 27 (1992) 3662–3666

Cyclic hardening and softening of Al–2.9% Cu–2.2% Mg–0.6% Mn alloy

Y. USTINOVSHIKOV
Physical-Technical Institute of the USSR, Academy of Science 132 Kizov Street, Izhevsk 426001, USSR

Electron microscopic research results are given for the Al–2.9% Cu–2.2% Mg–0.6% Mn alloy structure after different operating times corresponding to cyclic hardening or cyclic softening. It is shown that cyclic hardening results in precipitation of S′ particles and cyclic softening results in three processes: dissolution of S′ particles, precipitation of S″ particles instead of S′ ones and/or formation of regions free from precipitates. The main fatigue crack passes through cyclic-hardened material only and the hardening phase is merely the S′ particles. Relations between structure, cyclic hardening, cyclic softening and accumulated cyclic deformation are observed.

1. Introduction

Both cyclic hardening and cyclic softening of Al alloys have been observed by various investigators. The following mechanisms were proposed: local over-ageing in the slip bands, dissolution of coherent and semi-coherent particles when reciprocating movement of dislocations through them occurs; disordering in precipitates being repeatedly intersected by dislocations; dissolution of precipitates; dislocation rearrangement in the particles–matrix boundaries, etc. It is considered that cyclic hardening may be caused by the following factors: the existence of fields of coherent deformation around the particles; differences in shear modulus of the matrix and particles; differences in stacking-fault energies of the matrix and particles; initiation of new interfaces at intersecting particles by dislocations; changes of slip systems around particles, etc. Regions depleted by precipitates are formed in the structure in the case of fatigue damage. Migration of grain boundaries, over-ageing, initiation of striations and fine slip may exist inside the depleted regions.

Nevertheless, inhomogeneity in precipitate distribution cannot completely explain the nature of cyclic hardening and cyclic softening processes. For example, according to Goritsky and Terentjev [1] it follows that at the beginning of loading, cyclic hardening occurs and then cyclic softening. They proposed that cyclic hardening at the beginning of cyclic loading takes place due to increasing dislocation density. This then provokes cutting intersection of the particles by dislocations and their dissolution, resulting in cyclic softening.

A different kind of cyclic hardening and softening was observed by Daskovsky *et al.* [2]. They used diffusional tenso-resistors based on (BiTe) Sb as indicators of accumulated cyclic deformation. Softening at the beginning of cycling is accounted for by the partial dissolution of the precipitates due to reciprocating movement of the dislocations through them. The softening period is not so great since precipitate dissolution is a process proceeding in a direction opposite to decrease of the chemical potential difference. The process of dissolution cannot develop deeply enough and cyclic hardening occurs again.

In the present paper we have investigated the structure of the Al age-hardenable alloy with 2.9% Cu, 2.2% Mg and 0.6% Mn after different life times in order to elucidate the reasons for cyclic hardening and softening.

2. Experimental procedure

The Al–2.9% Cu–2.2% Mg–0.6% Mn alloy was dissolved at 500 + 3 °C for 30 min and quenched into water. The specimens were then aged for 16 h at 170 °C. The alloy is usually employed for compressor blades of gas-turbine aircraft engines in the Soviet Union. Investigations were therefore carried out in the initial state and after operating times of 1650, 3150, 8500 and 13 000 h, the latter being the maximum service life of the blades. In every state thin foils were obtained for electron microscopy. A blade cycled for 13 000 h was exposed to additional symmetric reverse bending cycling at $\sigma_{max} = 90$ MPa. After 30 000 cycles a main fatigue crack had appeared and specimens for electron microscopy were taken from the crack surface. The foils for electron microscopy were treated in 50% methanol and 50% nitric acid electrolyte. Rockwell B hardness measurements and X-ray measurements of lattice distortions were made as well.

3. Results

The cyclic hardening curves for the alloys investigated after different operating times are shown in Fig. 1. In spite of some scatter of the experimental points it is obvious that cyclic hardening and softening processes take place in the alloy. X-ray measurements of the lattice distortions also confirm their presence.

0022–2461

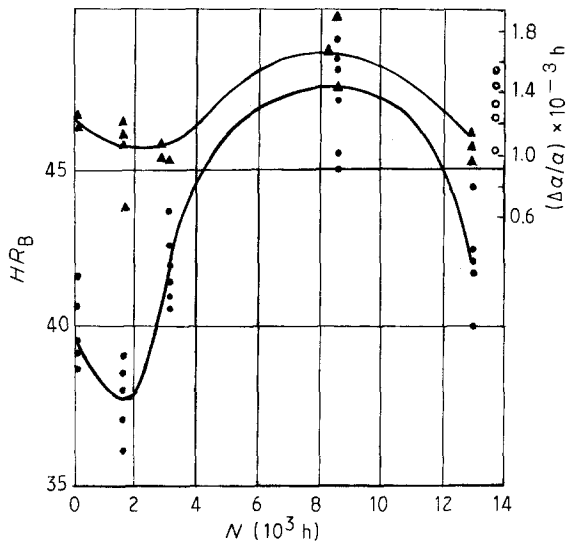

Figure 1 (●) Hardness HR_B and (▲) lattice distortion $\Delta a/a$ versus operating time N of the blades; (○) HR_B of a blade after 13 000 h of operating time and 30 000 cycles at $\sigma_{max} = 90$ MPa.

The correlation between the changes of both hardness and lattice distortion testifies that cyclic hardening and softening occur owing to the instability of hardening-phase particles, but not owing to dislocation density changes and dislocation rearrangement. Here we discuss the changes in the hardness and lattice distortion curves together with the electron microscopic investigations of the structure.

The structure of the alloy in the initial state is represented in Fig. 2a. Several types of precipitate are seen in the picture. Large particles having irregular forms (like the one marked A) are the equilibrium S-phase. The particles are not penetrated by the electron beam and, therefore, do not have their own spots in the electron diffraction patterns. Needle-like particles (like that marked B) are arranged in the ⟨1 0 0⟩ directions of the matrix. The electron diffraction pattern obtained from a region in which the B particles are present shows the lattice of these particles to be orthorhombic with $a = 0.405$ nm, $b = 0.906$ nm, $c = 0.720$ nm; i.e. these particles are the S′ phase (Fig. 2b). The orientation relationship between the matrix and the S′ precipitates is given as follows: $(1\,0\,0)_{Al} \parallel (2\,1\,0)_{S'}$, $[0\,1\,0]_{Al} \parallel [1\,2\,0]_{S'}$. The dark-field image of S′ phase particles received in the light of the additional spots indicated by the arrow in Fig. 2b is presented in Fig. 2d.

Along with the S and S′ phases, small particles arranged compactly in the ⟨1 0 0⟩ directions are seen in regions such as that marked C in Fig. 2a. The electron diffraction pattern obtained from the C region (Fig. 2e) differs from that obtained from the B one. Additional spots are spaced along the ⟨1 0 0⟩ directions of the matrix. This testifies to coherency between the matrix and the particles, and the coherent stresses are rather high. The electron diffraction pattern shows the C particles to be the S″ phase or the Guinier–Preston–Bagarjatsky-2 (GPB-2) zones. Their structure is ordered. In some cases the S″ phase particles decorate dislocations such as the one marked by D in Fig. 2a.

After 1650 h of operating time the hardness of the alloy is reduced. Lattice distortions also tend to fall (Fig. 1). Some changes take place in the alloy (Fig. 3): the S′ phase is not often observed in the electron micrographs and the number of S″ phase particles increases, these being distributed in the structure irregularly. In some cases the particles lie across the dislocation lines in the ⟨1 0 0⟩ directions. The S phase remains without changes. It is obvious that after 1650 h of cycling time the dissolution process of the S′ phase particles proceeds. As a result the number of S″ phase particles increases and regions free from precipitates appear. This indicates that dissolution of the S′ particles can be assumed to be the reason for the hardness decrease.

After 3150 h of cycling time the hardness of the alloy increases. The lattice distortions also have a tendency to intensify in comparison with 1650 h of cycling time. The structural changes are illustrated in Fig. 4. S′ phase particles are seen in the structure again. Their sizes are smaller than in the initial state and their arrangement looks like those of the S″ phase particles in the previous case. This allows us to assume that the S′ phase particles are formed at the points where the former S″ particles were arranged, that is, the S′ phase particles are formed through reconstruction of the S″ lattice into that of S′. The single spots of the S′ phase particles do not form a satellite system in the electron diffraction patterns as in the initial state (Fig. 4, inset). Therefore, the hardness increase after 3150 h of cycling time is supposed to be caused by the appearance of S′ phase particles in the structure.

After 8500 h of cycling time both the hardness and the lattice distortions of the alloy achieve a maximum (Fig. 1). As a rule, S′ phase particles are observed in the structure (Fig. 5). Their sizes are identical to those in the initial state. Naturally, the S phase particles exist without changes. The number of S″ phase particles is small, so they do not give their own spots in the electron diffraction patterns. Thus, one can suppose the structure of the S′ phase particles regularly arranged along the 1 0 0 directions of the matrix to be the most effective hardener of the alloy.

After 13 000 h of cycling time the hardness and the lattice distortions of the alloy are reduced in comparison with the preceding state but remain at a higher level compared to the initial state. The S′ phase particles exist in the structure but, however, their form, sizes and arrangement have undergone changes (Fig. 6), a study of which permits us to conclude that the S′ phase particles dissolve. During the dissolution process, long helicoidal dislocations are formed and some parts of them are decorated by precipitates. The presence of such dislocations in the structure usually testifies to the existence of a precipitate dissolution process. Regions free from precipitates are also present (Fig. 6).

The hardness of the alloy after 13 000 h of service time and 30 000 cycles of fatigue loading up to the appearance of the main fatigue crack is also shown in Fig. 1. It is the same near the crack and far from it. The hardness of the alloy having a crack is higher than that of the alloy in any other state. The S′ phase is the main

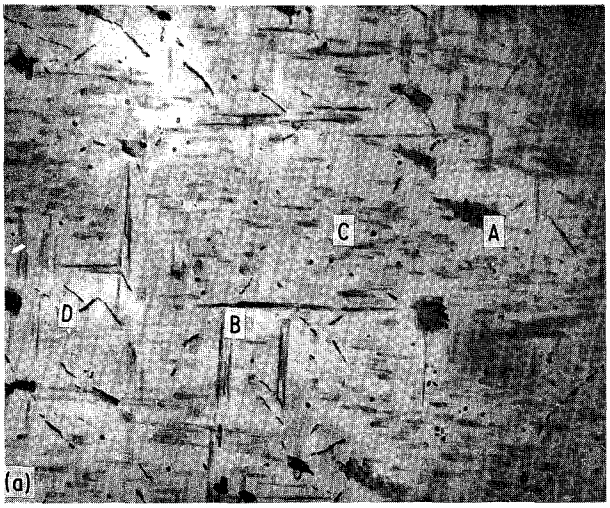

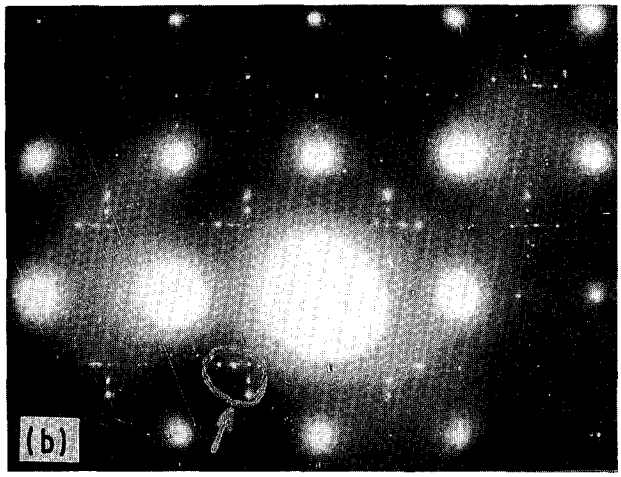

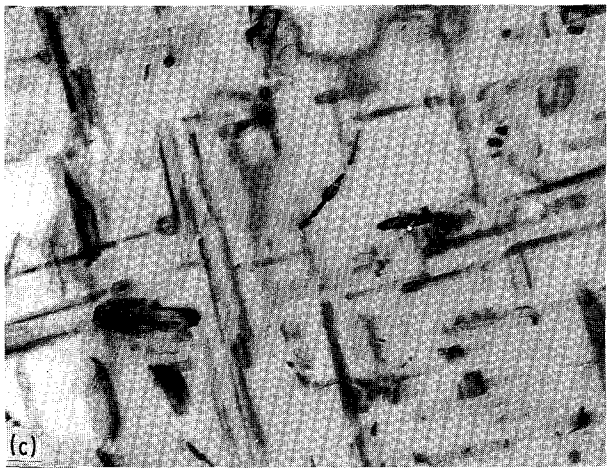

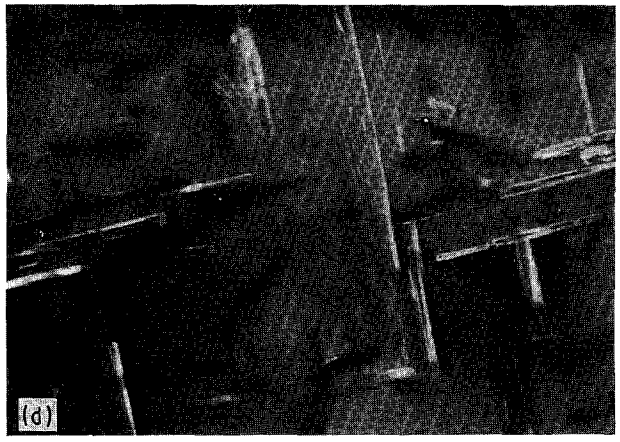

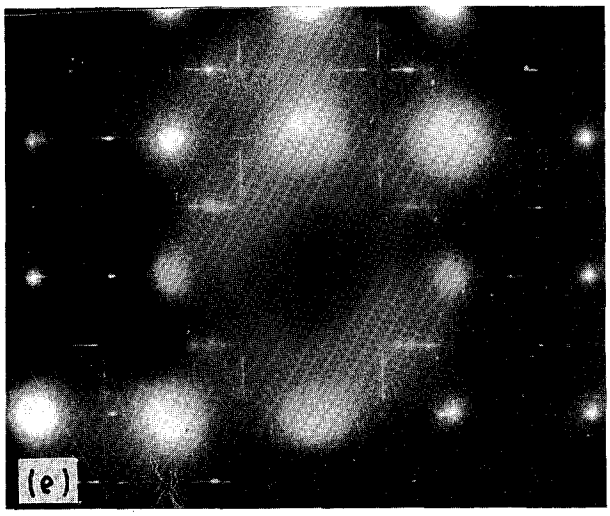

Figure 2 The structure in the initial state: (a) bright field, ×36 000; (b) electron diffraction pattern from the B region in (a); (c) bright-field and (d) dark-field images of the S′ phase, ×88 000; (e) electron diffraction pattern from the C region in (a).

hardener in the structure (Fig. 7). The latter circumstance testifies that the main fatigue crack initiates and spreads in the material when its maximum hardening state is attained, i.e. when the hardener is the S′ phase. Therefore, if a material is in cyclically non-hardened state, the main fatigue crack cannot occur.

4. Discussion

In numerous investigations it has been found the plastic deformation accumulation process leads always to fatigue failure. The kinetics of the accumulation process can be represented by the generalized curve $\Delta R/R_0 = f(N)$ (Fig. 8) derived by Daskovsky *et al.* [2] for Al age-hardenable alloys, independent of the type of hardened phase (GP zones in 2024 alloy, or S′ and S″ phases in 2618 alloy). Knowing the gauge factor of a strain gauge the $\Delta R/R = f(N)$ curve

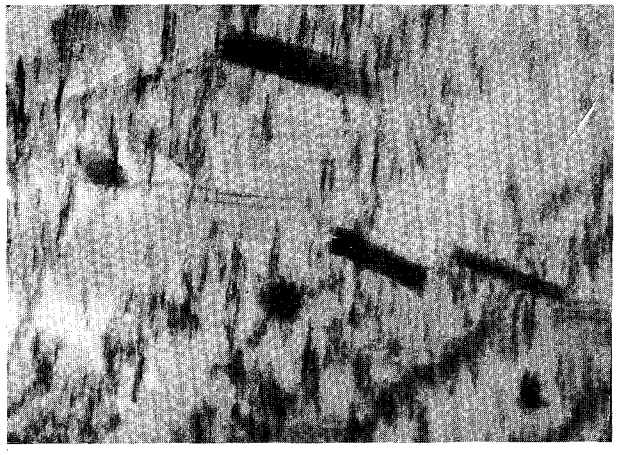

Figure 3 The structure after 1650 h of operating time. Bright field, ×88 000.

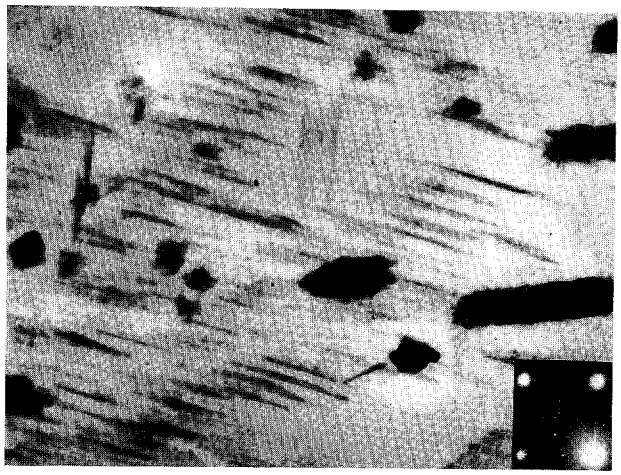

Figure 4 The structure after 3150 h of operating time. Bright field, ×88 000.

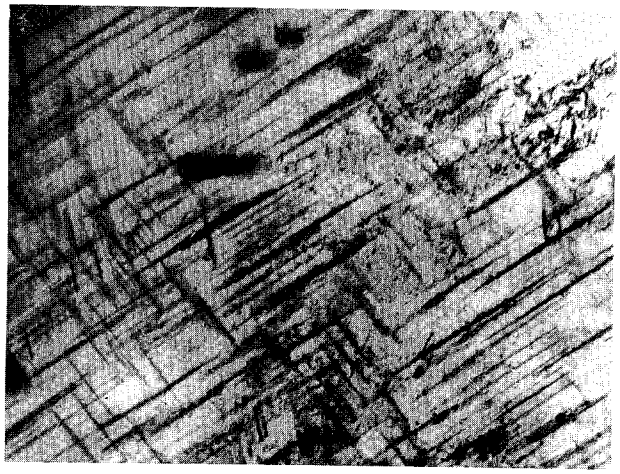

Figure 7 The structure after 13 000 h of operating time and 30 000 cycles at $\sigma_{max} = 90$ MPa on the surface of the fatigue crack. Bright field, ×88 000.

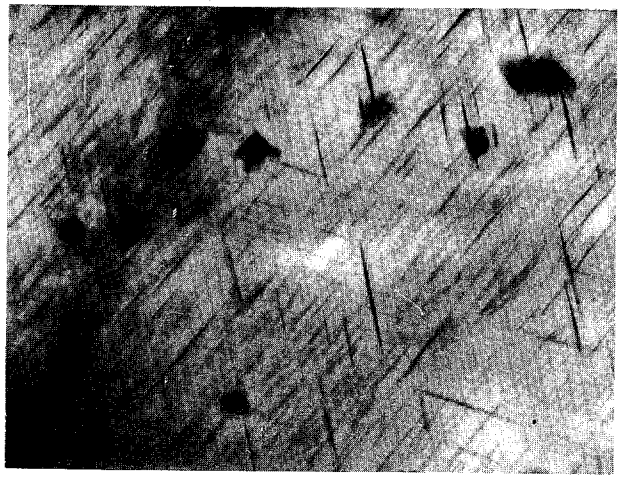

Figure 5 The structure after 8500 h of operating time. Bright field, ×88 000.

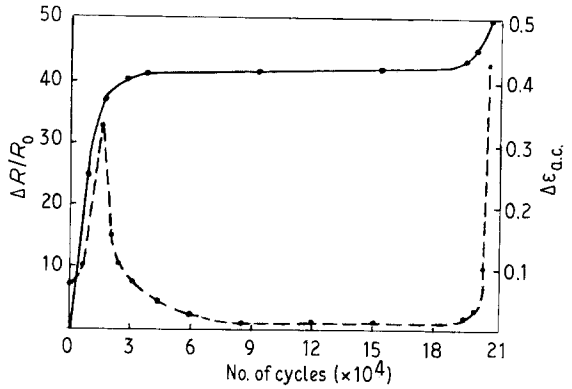

Figure 8 (——) Relative electrical resistance of gauges ($\Delta R/R_0$) and (– – –) amplitude of accumulated cyclic deformation per cycle, $\Delta\varepsilon_{a.c.}$, versus number of cycles of the Al age-hardenable alloy specimen at $\sigma_{max} = 170$ MPa [2].

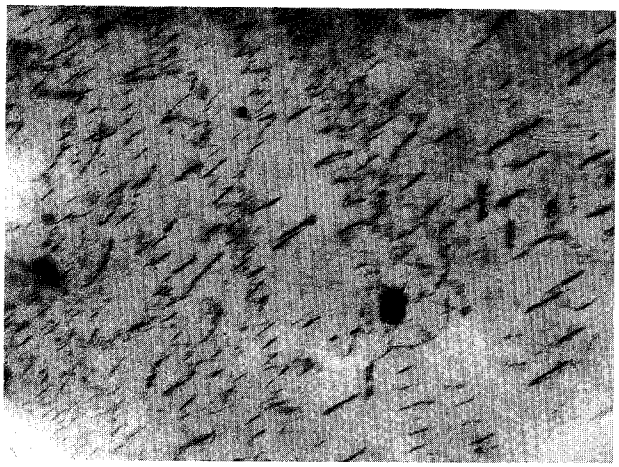

Figure 6 The structure after 13 000 h of operating time. Bright field, ×88 000.

can be reformulated as $\varepsilon_{\text{cyclic plastic}} = f(N)$. Then by differentiating the latter graphically the dependence of the change of accumulated cyclic deformation amplitude per cycle ($\Delta\varepsilon_{a.c.}$) on the number of cycles (dotted curve in Fig. 8) is obtained. Initially, the alloys are seen to undergo significant softening accompanied by sufficiently high growth of the accumulated cyclic deformation. Then cyclic softening is replaced by cyclic hardening, the value of which gradually decreases with the time of cycling. However, at the final stage of the fatigue process before the initiation of the main fatigue crack the softening repeatedly occurs. Fig. 1 of the present paper shows an analogous picture of the process: softening at the beginning of the time of cycling, then hardening for a long time, and while attaining maximum hardness the softening process repeatedly takes place. The electron microscopic results explain the reasons for these changes:

1. The initial cyclic softening accompanied by an increase of the accumulated cyclic deformation amplitude per cycle is determined by dissolution of the S′ particles and additional precipitation of the S″ particles in the structure.

2. Subsequent cyclic hardening, accompanied by a significant decrease of the cyclic deformation amplitude per cycle almost to zero, occurs due to the precipitation of S′ particles and the dissolution of S″ ones in the structure.

3. Repeated cyclic softening at the end of the fatigue life, accompanied by increasing cyclic deformation

amplitude per cycle, is observed as a result of the dissolution of S′ particles and the formation of regions free from precipitates.

4. The main fatigue crack results in local hardening of cyclically softened material in the regions wherein the crack spreads.

To summarize, instability of the hardening phases in Al age-hardenable alloys determines the exchange of the cyclic hardening and cyclic softening processes that prevent or promote accumulation of cyclic plastic deformation in alloys. The latter is a parameter from the value of which it is possible to evaluate the degree of fatigue life exhaustion in an alloy.

References

1. V. GORITSKY and V. TERENTJEV, "Structure and Fatigue Failure of Metals" (Metallurgy Press, Moscow, 1980).
2. I. DASKOVSKY, V. LYS and Y. USTINOVSHIKOV, *Problems of Strength* (Naukova Dumka, Kiev) No.10 (1987) 111.

Received 12 March
and accepted 1 July 1991